Optical and Quantum Electronics (2020) 52:483
https://doi.org/10.1007/s11082-020-02606-z

Optical, electrical, mechanical properties of Pr^{3+} and Yb^{3+} doped phosphate glasses

A. V. Deepa[1] · P. Vinothkumar[2] · K. Sathya Moorthy[2,5] · P. Muralimanohar[2] · Manoj Mohapatra[3,4] · S. Praveenkumar[6] · Priya Murugasen[2]

Received: 15 January 2020 / Accepted: 14 October 2020 / Published online: 24 October 2020

Abstract
The rare earth Pr^{3+} and Yb^{3+} doped phosphate glass were prepared by quenching method using electrical muful furnace. The optical band gap of rare earth Pr^{3+} and Yb^{3+} doped phosphate glass were studied. The dielectric permittivity, dielectric loss and electrical conductivity of the prepared samples have been studied using LCR meter with different frequencies at room temperature. The Vickers hardness number, brittle index, yield strength, fracture toughness of the rare earth Pr^{3+} and Yb^{3+} doped phosphate glasses were also calculated. The nonlinear optical parameters such as third order nonlinear coefficient and nonlinear refractive index were estimated using Z-scan method. The magnetic property of the Pr^{3+} and Yb^{3+} doped phosphate glass was studied using VSM analysis. The electro chemical properties of Pr^{3+} and Yb^{3+} doped phosphate glass electrodes in 5 M KOH electrolyte were studied using cyclic voltammetry, Galvanostatic charge–discharge and electrochemical impedance spectroscopy. The specific capacitance, energy density and capacity retention of Pr^{3+} and Yb^{3+} doped phosphate glasses were calculated.

Keywords Phosphate glass · Rare earth · Optical nonlinearity · Nonlinear susceptibility · Vickers hardness · Refractive index

✉ Priya Murugasen
priyam7373@gmail.com

1 Department of Physics, SNDP YSS COLLEGE, Kunnappally, Perinthalmanna, Malappuram, Kerala, India

2 Department of Physics, Saveetha Engineering College, Thandalam, Chennai 602105, India

3 Radiochemistry Division, Bhabha Atomic Research Centre (BARC), Trombay, Mumbai 400 085, India

4 Homi Bhabha National Institute, Anushakti Nagar, Mumbai 400 094, India

5 Department of Physics, Presidency College, Affiliated to University of Madras, Chennai 600 005, India

6 Department of ECE Saveetha Engineering College, Thandalam, Chennai 602105, India

1 Introduction

Glass is an inorganic solid material, which is transparent at room temperature. Glass is a name given all amorphous materials which can be obtained by lowering the temperature of melt, independently of its chemical composition ant its temperature range of solidification. When a liquid is cooled to solid state, there is a possibility of getting two outputs (i) glassline materials (ii) amorphous materials. In glassy materials, the constituent particles are arranged in a random manner and lack the long range periodic glass structure.

Eg: Glass, Rubber and Plastic. The amorphous materials show short range periodicity. In past decades, peoples used glasses for making ornaments with the unawareness of its properties.

But in present century glasses attain prior position in both optical and communication field with its emerging trends in latest technologies. In our daily life, glasses are used for numerous applications. For example, glass components are used in medical diagnostic equipments. Normally pure silica is being used as the raw material for glass preparation.

Due to the high melting point of silica and other disadvantages many researchers have changed the basic components of making glass and focused on the preparation of non-silicate glasses (network glasses, oxide glasses) like borate glasses, phosphate glasses, alumina silicate glasses, etc.

The three components of oxide glasses are glass former, intermediate and modifier. Instead of silica, one can choose oxides of elements as glass formers. This oxides exhibit intermediate electro negativity, which forms glass of their own. Eg: B_2O_3, P_2O_5 etc. Intermediates do not form glass itself but helps in the formation of glasses. The cation of intermediate is capable of entering into the glass network and occupies the position of glass former. Eg: Zn, Ti. The Modifier (Eg: Li, Na) forms glass, only when it mixed in correct proportion with glass former. By the addition of modifier, the continuous glass network is disrupted.

The famous scientist Goldschmidt framed some rules to select a glass former. They are (i) Glass forming oxides are those for which the ratio of ionic radii of anions and cations lies in 0.2 to 0.4 (ii) 4 anions are surrounded to each cation. Anions should be situated at corners, ie.triangular configuration is must. Later Zachariasen agrees this with some modifications:

(i) Oxygen coordination should be less normally 3 or 4.

(ii) Sample contains high percentage of cation which are surrounded by oxygen tetrahedral or trigonal (Shelby 2020).

In the present work we have concentrated on phosphate glasses. In phosphate glass, P_2O_5 is considered as glass former. The phosphate glass is a class of optical glass composed of metaphosphate of various metals. While comparing to borate glasses, in phosphate glasses oxygen is non-bridging.

The Phosphate glasses exhibits in sheet form and consists of layers of oxygen polyhedral with weak Vaan der Waals force of attraction between the layers. The rigidity of the structure can be modified by the addition of alkali or alkaline earth elements (Sharaf et al. 2008). The Phosphate glasses are more superior than silicate glasses in practical conditions due to their low melting point high refractive index and good rare earth solubility. While comparing with others, they are high resistance to hydrofluoric acid. They show low resistance to chemical corrosion. The phosphate glasses are well suited for doping with various elements like transition metals and rare earth elements.

The Rare earth elements are taken as dopants in prepared samples. The lanthanides are known as Rare earth elements. These elements are not occur commonly in earth and difficult to separate each other. Usually RE elements are trivalent. Lanthanides are d-block elements. Among the seventeen RE elements, Praseodymium and Ytterbium are chosen as dopants.

The Praseodymium is used to make specialized yellow glasses for glass welders. On the basis of this concept, the Pr^{3+} doped phosphate glasses were synthesized and characterized.

Ytterbium is more reactive than other lanthanides. Ytterbium is used for making lasers. The primary application of ytterbium doped glass lasers is in material processing like welding, cutting etc. The ytterbium doped glasses finds use as active medium for lasers. The ytterbium is popular for their NIR luminescence, while Pr^{3+} show transitions in the NIR region. In this present paper have been reported the linear and Nonlinear optical, mechanical and electrical properties of Pr^{3+} and Yb^{3+} doped phosphate glasses.

2 Sample preparation

Glasses are formed through several processes but the most common method is melt quenching. In this technique, the raw material is heated to molten state and then rapidly cooled to solid state. All the raw materials are melted at ambient temperature.

All the raw materials (Sigma Aldrich, 99.99%, purity) were weighted in correct proportion based on the batch formula, grinded and mixed using electric mortar for 15 min to get fine powder mixture. The prepared samples were taken in crucible and kept in a furnace which was maintained at 1400 °C for 4–5 h. After continuous monitoring, the melt is transferred to another furnace for annealing when melting process gets over. The as prepared Yb^{3+} and Pr^{3+} doped phosphate glasses are shown in Fig. 1a, b.

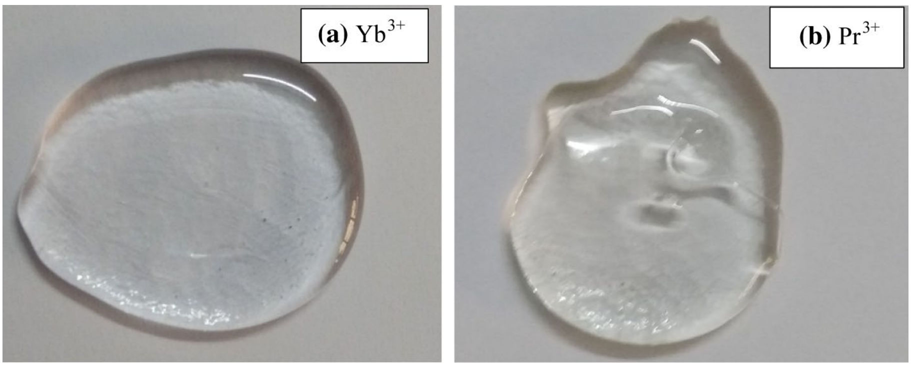

Fig. 1 As prepared (a) Yb^{3+} and (b) Pr^{3+} doped phosphate glass

3 Characterization

3.1 Fluorescence emission spectra

The fluorescence spectra of rare earth Pr^{3+} and Yb^{3+} doped phosphate glass have been recorded by using time correlated Single Photon counting instrument (purchased from Horiba Jobin Yvon, USA, NJ). The Fluorescence spectroscopy deals with electronic and vibrational states. The energy level $^3H_4$ is ground state of Pr^{3+}. In order to record the emission spectra, the radiations have been excited to 390 nm.Several weak intense emission bands appeared in the graph. Four peaks observed in the range 480–560 nm region are distinct.

The sharp features are absent in the optical spectra of amorphous materials. The transitions such as $^3P_0$-$^3H_4$, $^3P_0$-$^3H_5$, $^1P_1$-$^3H_5$, $^3P_0$- $^3H_6$ and their wavelengths are 485,510,540 and 560 nm respectively. An emission band at 485 nm attains comparatively more intense peak.

The two transitions like $^3P_0$-$^3H_5$, $^1P_1$-$^3H_5$ occurred in 520–560 nm range and their influence in total fluorescence is very small (Sharma et al. 2000; Rupa et al. 2018). The fluorescence spectra of and Pr^{3+} and Yb^{3+} doped phosphate glass is shown in Fig. 2 and 3. The absorption and emission spectra were drawn in same graph with black and red color respectively.

Normally Yb can be used as an acceptor because it exhibits only two energy levels $^2F_{7/2}$ and $^2F_{5/2}$. The level $^2F_{7/2}$ is the ground energy level and $^2F_{5/2}$ is excited level. The energy of excited Yb ions are very close to the band gap of silicon and its luminescence quantum efficiency is maximum in NIR region. On account of these properties, Yb can be used in memory devices, tunable lasers and also as industrial catalyst. The broad absorption and emission of Yb^{3+} ions are due to electronic transitions involving the Stark sublevels. From the measurement, the emission spectra of Yb^{3+} doped phosphate glass shows maximum intensity at 978 nm which indicates the $^2F_{7/2}$—$^2F_{5/2}$ transition.

The Optical properties of Pr^{3+} and Yb^{3+} doped phosphate glasses were explained by UV–Vis spectroscopy. The resultant absorption spectrum recorded with Perkin Elmer

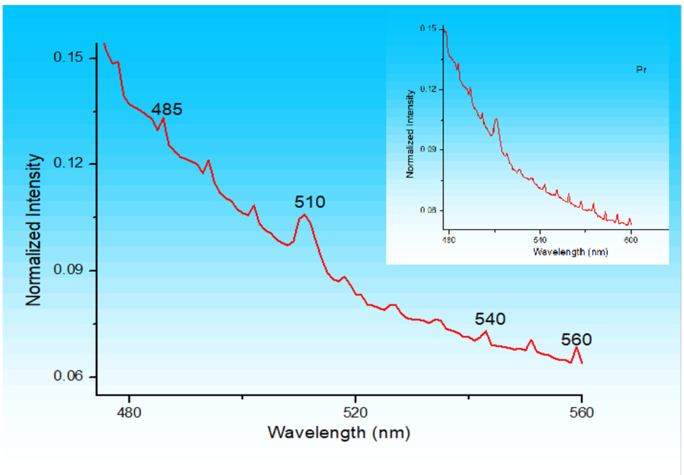

Fig. 2 Fluorescence emission spectra of Pr^{3+} doped Phosphate glasses

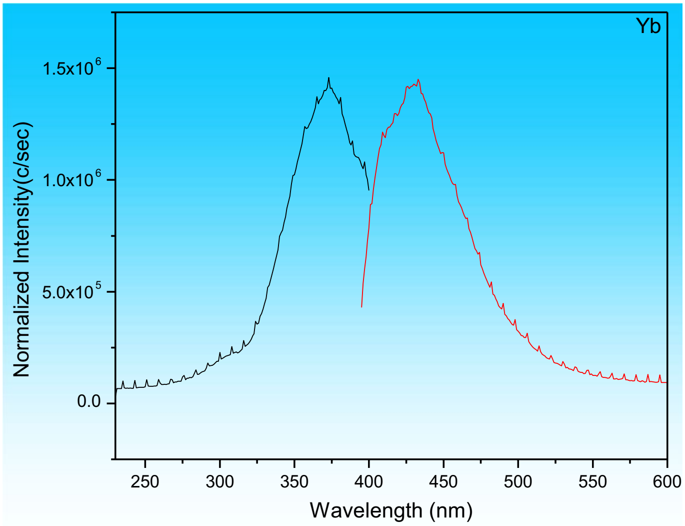

Fig. 3 Fluorescence emission spectra of Yb^{3+}doped Phosphate glasses

Lambda 1050 spectrophotometer, in the range of 200–800 nm and Pr^{3+} doped phosphate glass is shown in Fig. 4.

The number of peaks with different wavelength are seen which is happens due to the electronic transition between the inner orbits of RE ions (Elisa et al. 2013). Also it doesn't show any sharp absorption edge, which supports the characteristics of glassy state. The absorption bands of Pr^{3+} are seen at 437 nm, 467 nm, 480 nm and 560 nm respectively. The corresponding transitions are from ground state $^3H_4$ to $^2P_3$, $^3P_1$, $^1P_0$, $^1D_2$ respectively. The earlier H. Zhang et al. has reported the similar transitions in their studies (Zhang et al. 1999). Similar absorption curve of Yb^{3+} doped phosphate glass are depicted in Fig. 5.

The excitation spectra of Yb does not shown any single sharp peak because the energy levels become split into small lines. The two 4f levels can split into 4stark lines

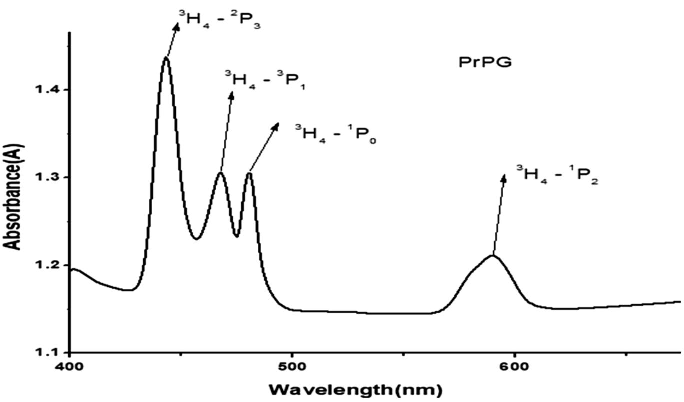

Fig. 4 UV –Visible spectrum of Pr^{3+} doped Phosphate glasses

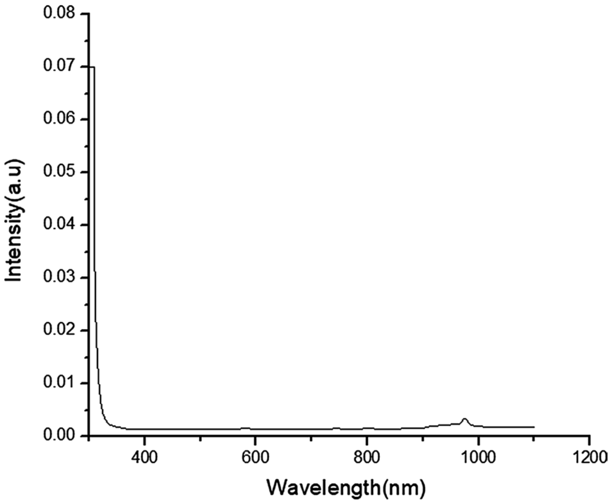

Fig. 5 UV –Visible spectrum of Yb^{3+} doped Phosphate glasses

for ground and 3 stark lines for excited state. Generally to attain this kind of spectral splitting in room temperature is tedious.

In low temperature measurements, the interaction between Yb ions with lattice vibrations are considered. The more vibrational transitions occur in the spectra due the interaction between electron and phonon. The Yb ions are located in various crystallographic sites because of the different values of the absorption coefficients (IR region).The stark lines are discriminated using Greek letters. The graph shows an excitation at 236 nm, which denotes Y-lines, another peak at 242 nm denotes Alpha line.

The spectra shows a large number of weak transitions also, which indicates the presence of impurities. Due to the difficulty of getting absorption spectra for powder samples in Infra-Red range, normally we can neglect the lowest part of the spectra.

The less absorption has been observed in the visible region and confirms that the quality of the glass is good. The required properties for NLO activity are minimum absorption and low cut-off wavelength.

The electrons are excited from a filled band to an empty one by photon absorption and shows a marked increases in the absorption coefficient.

The optical absorption coefficient (α) was calculated using the following relation (Krishnakumar and Nagalakshmi 2005; Yakuphanoglu and Erten 2005).

$$\alpha = \frac{2.3026 \log\left(\frac{1}{T}\right)}{t} \tag{1}$$

where T is the transmittance and d is the thickness of the glass. The various other optical constants were calculated using the following theoretical formulae. The energy dependence of the absorption coefficient suggests the occurrence of direct band gap and hence it obeys the relation for high photon energy.

$$(\alpha h\upsilon)^2 = \mathrm{A}\left(\mathrm{E_g} - \mathrm{h}\upsilon\right) \tag{2}$$

where E_g is the optical band gap and A is a constant.

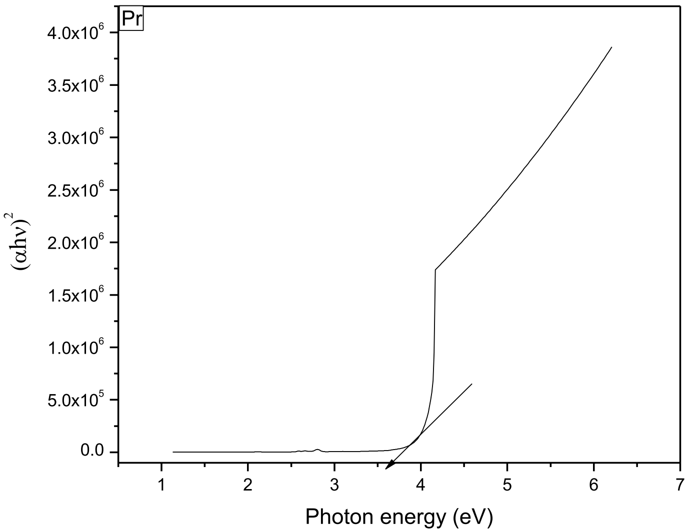

Fig. 6 Photon energy verses $(\alpha h\upsilon)^2$ of Pr^{3+} doped phosphate glass

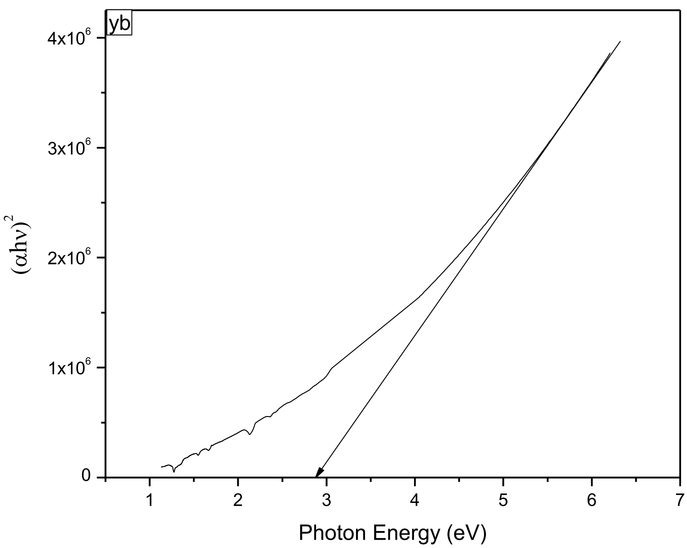

Fig. 7 Photon energy verses $(\alpha h\upsilon)^2$ of Yb^{3+} doped phosphate glass

The variation of $(\alpha h\upsilon)^2$ versus photo energy in the fundamental absorption region are plotted in the Figs. 6, 7 for Pr^{3+} and Yb^{3+} doped phosphate glasses. E_g is examined by the extrapolation of the linear part. The optical band gap of Pr^{3+} and Yb^{3+} doped phosphate glasses were found to be 3.6 eV and 3.0 eV respectively.

The extinction coefficient is obtained in terms of the absorption coefficient,

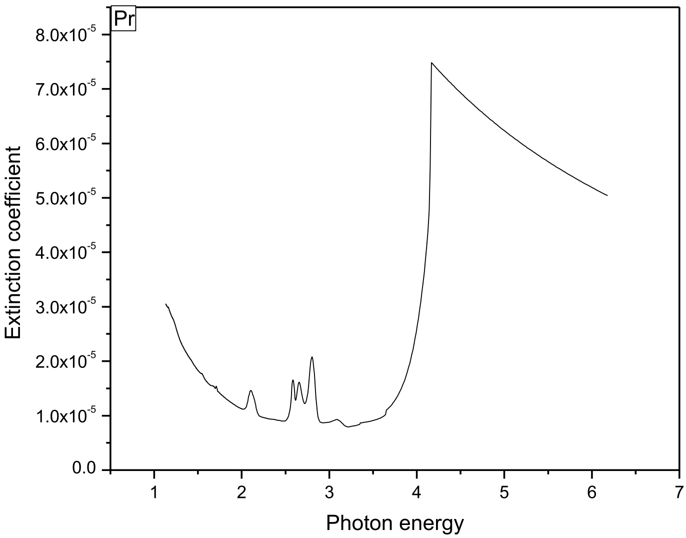

Fig. 8 Photon energy verses Extinction coefficient of Pr^{3+} doped phosphate glass

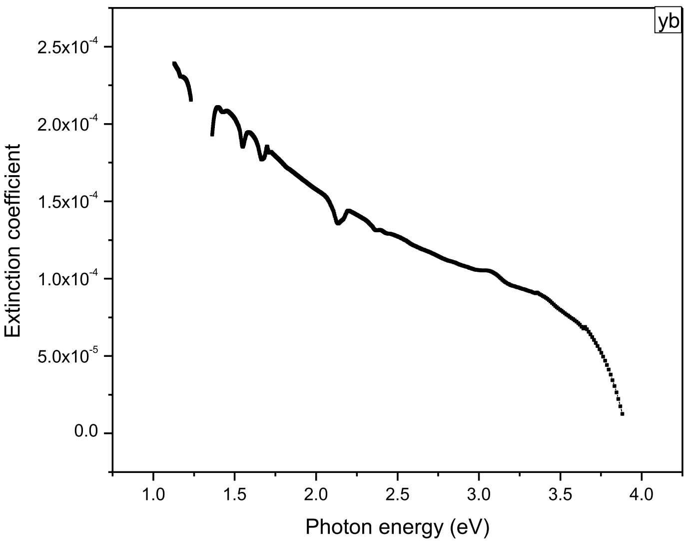

Fig. 9 Photon energy verses extinction coefficient of Yb^{3+} doped phosphate glass

$$K = \frac{\alpha\lambda}{4\pi} \tag{3}$$

The photon energy versus extinction coefficients of Pr^{3+} and Yb^{3+} doped phosphate glasses are shown in Figs. 8 and 9 respectively. The extinction coefficients of Pr^{3+} and Yb^{3+} doped phosphate glasses were found to be 1.107161×10^{-5} and 8.412×10^{-5} at 3.5 eV respectively.

The reflectance in terms of the of absorption coefficient is derived,

$$R = \frac{\exp(-\alpha t) \pm \sqrt{\exp(-\alpha t)T - \exp(-3\alpha t)T + \exp(-2\alpha t)T^2}}{\exp(-\alpha t) + \exp(-2\alpha t)T} \tag{4}$$

The glass refractive index has a main dependency on two kinds of transmissions, they are.

(i) Anion and cations that are bridging and non-bridging in the UV region.
(ii) The vibrations of the lattice in glass networks in the region of infrared.

The linear refractive index is given by

$$n = -(R+1) \pm 2^9 \frac{\sqrt{R}}{(R-1)} \tag{5}$$

Figures 10 and 11 show the photon energy verses refractive Index of Pr^{3+} and Yb^{3+} doped phosphate glasses. The refractive index (n) of Pr^{3+} and Yb^{3+} doped phosphate glasses were estimated and found to be 1.54 and at 1.4833 eV respectively.

From the optical constants, electric susceptibility (χ_c) can be calculated according to the following relation.

$$\chi_c = \frac{n^2 - k^2 - \varepsilon_o}{4\pi} \tag{6}$$

where ε_o is the dielectric constant. The value of electric susceptibility (χ_c) of Pr^{3+} and Yb^{3+}doped phosphate glasses were calculated and found to be 0.1654 and 0.3390 at λ=600 nm.

Also the complex dielectric constant is related to the refractive index and the extinction coefficient as

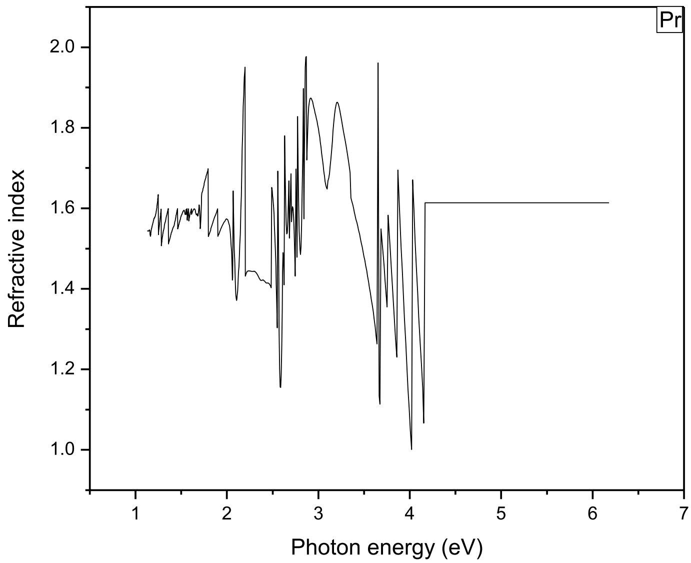

Fig. 10 Photon energy verses refractive Index of Pr^{3+} doped phosphate glass

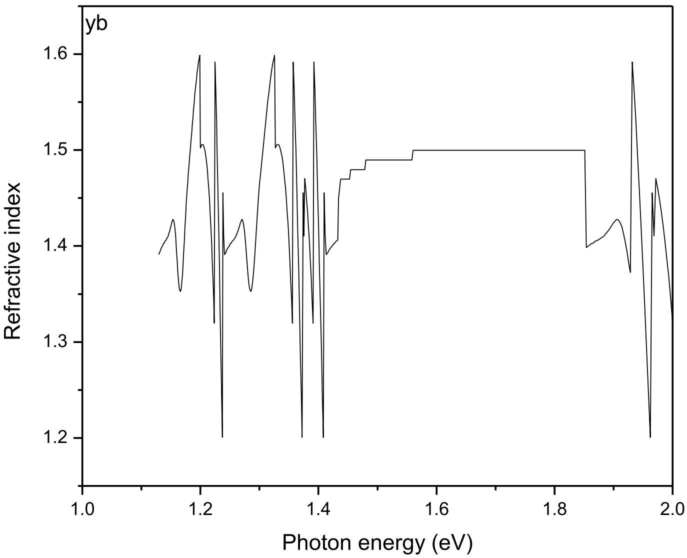

Fig. 11 Photon energy verses refractive index of Yb^{3+} doped phosphate glass

$$\varepsilon_c = \varepsilon_r + \varepsilon_i \tag{7}$$

The value of real dielectric constants of Pr^{3+} and Yb^{3+} doped phosphate glasses are found to be 3.0779×10^{-5} and $6.\ 4957 \times 10^{-5}$ and imaginary dielectric constants are 0.0059 and 0.0044 at $\lambda = 600$ nm respectively, where the real and imaginary dielectric constant are

$$\varepsilon_r = n^2 - K^2 \tag{8}$$

$$\varepsilon_i = 2nK \tag{9}$$

The optical conductivity is a measure of the frequency response of the material when irradiated with light (Lucarelli et al. 2002; Ugwu et al. 2009).,which is given by

$$\sigma_{op} = \frac{\alpha nc}{4\pi} \tag{10}$$

where c is the velocity of light. The electrical conductivity can also be estimated by optical method using the relation

$$\sigma_e = \frac{2\lambda\sigma_{op}}{4\pi} \tag{11}$$

Figure 12 and 13 shows the variation of the electrical conductivity as a function of photon energy for the rare earth Pr^{3+} and Yb^{3+} doped phosphate glass samples respectively.

The extinction coefficient changes accordance with that photon energy suggest the extinction coefficient decreases with energy and inverse dependence with E.

Figures 14, 15 show the variation of the optical conductivity as a function of photon energy for the rare earth Pr^{3+} and Yb^{3+} doped phosphate glass sample respectively. It can

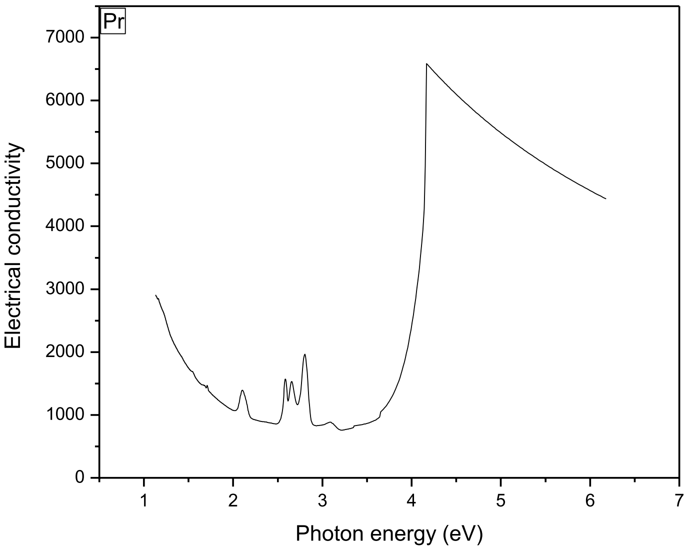

Fig. 12 Photon energy verses Electrical conductivity of Pr^{3+} doped phosphate glass

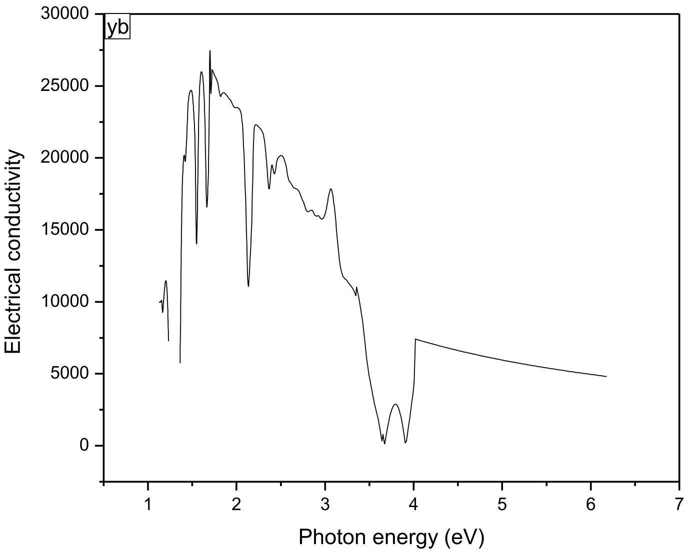

Fig. 13 Photon energy verses electrical conductivity of Yb^{3+} doped phosphate glass

be seen clearly that the optical conductivity directly depends on the absorption coefficient and the refractive index of the material.

The high transmission, low absorbance, low reflectance and low refractive index of rare earth Pr^{3+} and Yb^{3+} doped phosphate glasses in the UV–Vis region make the material a prominent one for anti-reflection coating in solar thermal devices and nonlinear optical application.

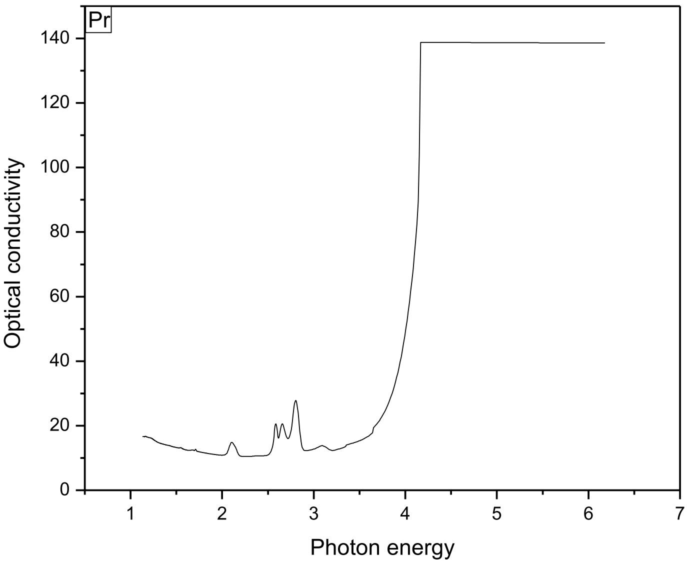

Fig. 14 Photon energy verses Optical conductivity of Pr^{3+} doped phosphate glass

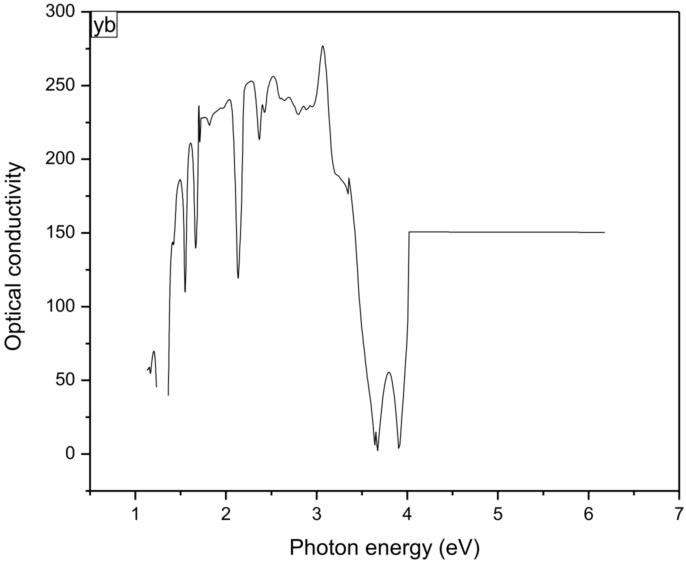

Fig. 15 Photon energy verses optical conductivity of Yb^{3+} doped phosphate glass

The low extinction value (10^{-3}) and electrical conductivity ($10^{2}\Omega cm^{-1}$) show the semiconducting nature of the material.

The high magnitude of optical conductivity confirms the presence of very high photo response nature of the material.

This makes the material more prominent for device applications in information processing and computing. The lower dielectric constant and the higher optical response suggest the better conversion efficiency of the material.

3.2 Dielectric studies

Rare earth Pr^{3+} and Yb^{3+} doped phosphate glass of desired size were selected for dielectric measurements. Silver paint was applied on opposite faces of cut and polished rare earth Pr^{3+} and Yb^{3+} doped phosphate glass to make a capacitor for investigation. The samples were mounted on a sample holder made of stainless steel. The dielectric measurements were carried out at the frequency range from 100 Hz to 5 MHz at various temperatures with the help of an impedance analyser. Then the dielectric constant of the sample as the function of frequency and temperature were further automated using a computer for data recording, storage and analysis.

The values of capacitance (C_p) and loss (tan δ) were obtained from the dielectric measurement. Other parameters such as dielectric constant and ε_r are calculated using the formula

$$\varepsilon_r = \frac{C_p t}{\varepsilon_0 A} \tag{12}$$

where t is the thickness of the sample, ε_0—permittivity of free space. *A*- The area of the sample, *f*—the frequency of applied field. Studies of temperature and frequency dependence of dielectric properties unveil useful information about structural changes, defect behaviour, and transport phenomena.

Figure 16 shows the frequency dependency of dielectric constant and dielectric loss for Pr^{3+} doped phosphate glass. The dielectric constant is maximum at low frequencies and decreases further with increasing frequency. It is evident from the measurement,

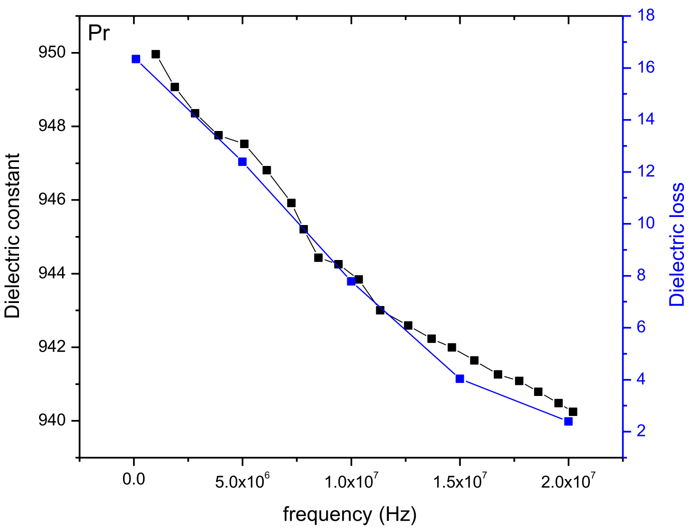

Fig. 16 Frequency verses dielectric constant and dielectric loss of Pr^{3+}doped phosphate glass

that the frequency of the electric field and the natural frequency of bound charges are equal. It results in the oscillation of the molecules with high energy.

At higher frequencies, the dielectric constant decreases due to the natural frequency of the bounded charge, moreover, at low frequencies all mechanisms such as space charge, orientation, ionic and electric polarization are operative, hence the ε_r is maximum (Valente et al. 2011; Sadhukhan et al. 1999).

Figure 17 shows the frequency dependency of dielectric constant and dielectric loss for Yb^{3+} doped phosphate glass. The dielectric constant is minimum at higher frequencies as all the mechanisms mentioned above do not follow the applied electric field. At this stage, the frequency of the applied electric field is not equal to the natural frequency of bounded charge. It is not an indication for spontaneous polarization.

The dielectric loss also exhibits similar behaviour for both as prepared glasses. Increase of dielectric loss at low frequencies is attributed to the oscillation of dipoles. At higher frequencies, all the polarization mechanism are not operative, hence energy need not to be spent rotate dipoles, therefore, dielectric loss is also minimum (Raja et al. 2004).

3.3 Third order nonlinear study

Measurement of optical nonlinearity was carried out by Single beam Z-scan technique with nanosecond laser pulses to measure rapidly both non-linear absorption (NLA), non-linear refraction (NLR), Nonlinear changes in index (Δn) and changes in absorption ($\Delta\alpha$) of phosphate glasses. To measure these parameter, 2 mm thick sample was analysed using 300 ns TEA CO_2 laser pulses having energy of 0.85 mJ.

The transmittance of the sample through the aperture is monitored in the far field as a function of the position 'Z' of the nonlinear sample in the vicinity of the linear optics

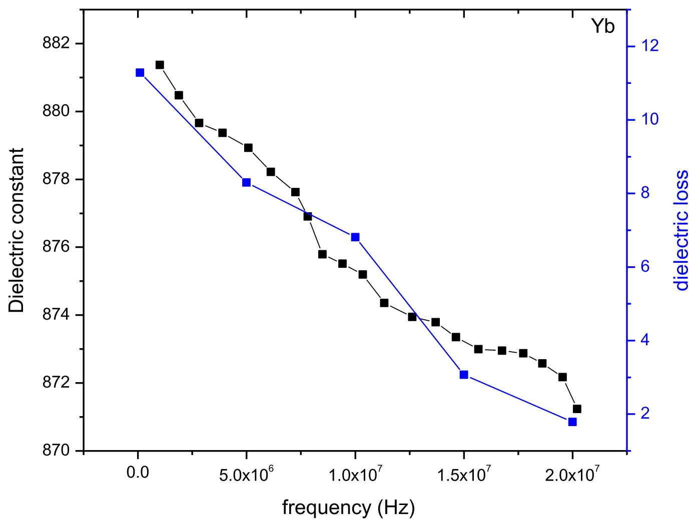

Fig. 17 Frequency verses dielectric constant and dielectric loss of Yb^{3+}doped phosphate glass

focal position. The required scan range in the experiment depends on the beam parameters and the sample thickness L. Critical parameter is the diffraction length 'Z_0' of the focused beam defined as $\pi\omega_0^2/\lambda$ for a Gaussian beam where ω_0 is the focal spot size.

From the closed aperture, $\Delta T_{p\text{-}v} = T_p - T_v$.

where T_p and T_v are the normalized peak and valley transmittances.

The empirically determined relation between the induced phase distortion, $\Delta\Phi_0$, and $\Delta T_{p\text{-}v}$ for the third-order nonlinear refractive process in the absence of NLA is (Sheik-Bahae et al. 1989).

$$\Delta T_{p-v} \cong 0.406(1-s)^{0.25}|\Delta\phi| \tag{13}$$

where $\Delta\phi = \frac{2\pi}{\lambda} n_2 I_o L_{eff}$

With, $L_{eff} = (1-e^{-\alpha L})/\alpha$, and $S = 1 - \exp\left(\frac{-2r_a^2}{\omega_a^2}\right)$, is the transmittance of the aperture in the absence of a sample. $\Delta\Phi_0$ and I_0 are the on-axis (r=0), peak (t=0) nonlinear phase shift and the irradiance with the sample at the focus (Z=0) respectively. The sign of $\Delta\Phi_0$ and hence n_2 is determined from the relative positions of the peak and valley with Z.

The above relation is accurate to within ±3% for $\Delta T_{p\text{-}v} < 1$. As an example, if the induced optical path length change due to the nonlinearity is λ/250, $\Delta T_{p\text{-}v} \approx 1\%$ for an aperture transmittance of S=0.5. Use of S=0.5 is a good compromise between having a large signal which averages possible beam non-uniformities, thus reducing background signals, and loss of sensitivity. Figure 18. Z/Z_o verses normalized transmittance for closed aperture and open aperture of Pr^{3+} phosphate glass. The nonlinear refractive index (n_2) and nonlinear absorption coefficient (β) are given by (Mojdehi et al. 2013),

$$n_2 = \frac{\Delta\phi}{K\, I_{o\, L_{eff}}} \tag{14}$$

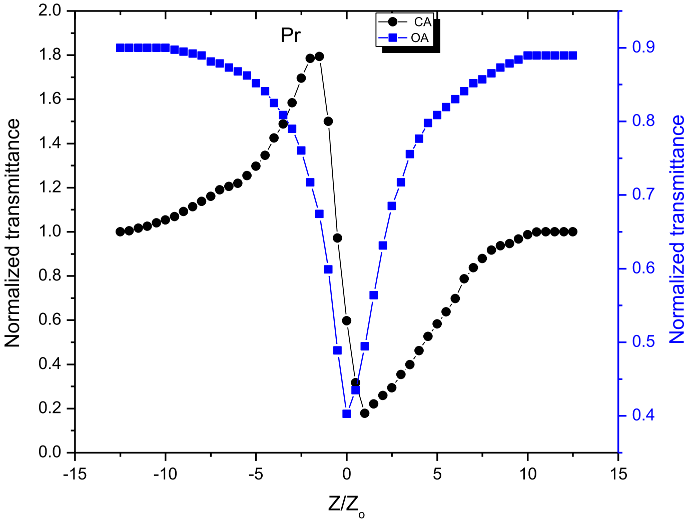

Fig. 18 Z/Z_o verses normalized transmittance for closed aperture and open aperture of Pr^{3+} phosphate glass

$$\beta = \frac{2\sqrt{2}\Delta T}{I_o\ L_{eff}} \tag{15}$$

where ΔT is the difference between the normalized transmittance at z = 0 and z → ∞ of the open aperture Z-scan. I_0 is the radiation intensity at the focal point, which is 5 W/cm^2. Figure 19 shows Z/Zo verses normalized transmittance for closed aperture and open aperture of Yb^{3+} phosphate glass. The NLO absorptive property of rare earth doped phosphate glasses indicate a positive sign for the nonlinear refraction and exhibits self-defocusing behaviour.

Then the effective third-order NLO refractive index nonlinear refractive index (n_2) and nonlinear absorption coefficient (β) of Pr^{3+} and Yb^{3+} doped phosphate glasses are estimated and listed in Table 1.

The real and imaginary parts of the third order nonlinear susceptibility χ3 are defined as,

$$Re\ \chi^3 = \frac{10^{-4}\left(\varepsilon_o C^2 n_o^2\right)}{3.14} esu \tag{16}$$

$$Im\ \chi^3 = \frac{10^{-2}\left(\varepsilon_o C^2 n_o^2 .\lambda.\beta\right)}{4\pi^2}\ esu \tag{17}$$

where ε_0 is the vacuum permittivity, n_o is the linear refractive index of the sample and c is the velocity of light in vacuum. Thus, we can easily obtain the absolute value of χ^3 by the following formula [32].

$$\chi^3 = \sqrt{\left(Re\chi^3\right)^2 + \left(Im\chi^3\right)^2}\ esu \tag{18}$$

The third order susceptibility (χ^3) of Pr^{3+} and Yb^{3+} doped phosphate glasses are found to be 11.3073 × 10^{-8} esu and 11.8078 × 10^{-8} esu respectively. Table 1 shows the

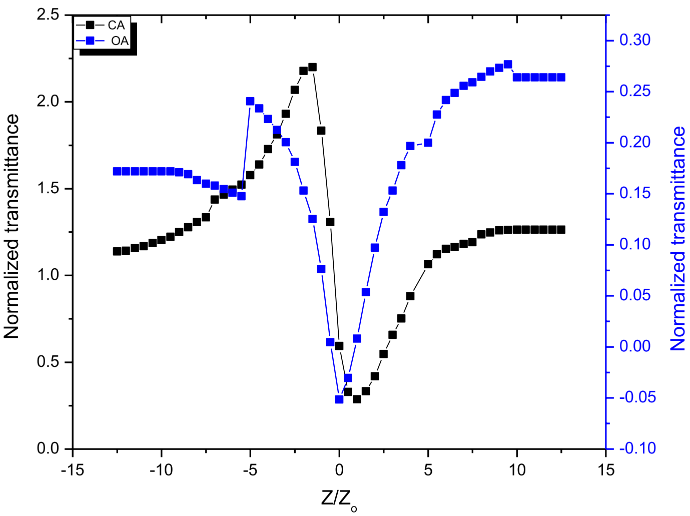

Fig. 19 Z/Z$_o$ verses normalized transmittance for closed aperture and open aperture of Yb^{3+} phosphate glass

Table 1 The Nonlinear optical parameters of Pr^{3+} and Yb^{3+} doped phosphate glasses

Sample	Alphamm^{-1}	$n_2 10^{-8}$ cm^2/W	$\beta 10^{-7}$ cm/mW	n_o	Re $\chi^{(3)}$ 10^{-6} esu	Im $\chi^{(3)}$ 0^{-6} esu	$\chi(3)$ 10^{-6} esu
Pr^{3+} doped phosphate glass	0.639	3.129	4.8992	1.6899	10.9003	2.8939	11.3073
Yb^{3+} doped phosphate glass	0.4893	2.8109	3.6410	1.6288	9.3802	2.5290	9.3802

experimental results of the Z-scan technique for prepared glasses. Z-scan measurement is important parameter because it is used to estimate and control refractive index gratings, which are significant for some laser based dynamic holography (Shanmugavelu and Venkatramu 2014).

3.4 Micro-hardness study

Hardness is the resistance offered by the glass for localized plastic deformation. This property is basically related to the glass structure of the material and the electronic factors operating to make the structure stable.

The micro hardness has been measured along the plane of the rare earth Pr^{3+} and Yb^{3+} doped phosphate glass at room temperature using Leitz–Wetzler hardness tester ranging from 10 to 200 g. The corresponding indentation length were measured. The Vickers micro hardness number (H_v) at each load was calculated using the relation (Sangwal 2009).

$$H_v = 1.8544\ P/d^2\left(Kg/mm^2\right) \tag{19}$$

where, H_v is the Vickers hardness number, P is the applied load and d is the average diagonal length of the indentation mark. The microhardness number varied with respect to applied load.

Figures 20, 21 represent load verses. hardness number and yield strength of Pr^{3+} and Yb^{3+} doped phosphate glass. It is seen that the hardness value increases with increasing load values up to 100 g, which is known as reverse indentation size effect (RISE). The crack was formed beyond 100 g. it is due to high stress required for homogeneous nucleation of dislocations in the small dislocation free region indented.

The yield strength of Pr^{3+} and Yb^{3+} doped phosphate glasses also increased with increasing load. The yield strength refer to the stress at which the materials begin to deform plastically and depends on the Meyer's index (n). It is calculated using the relation,

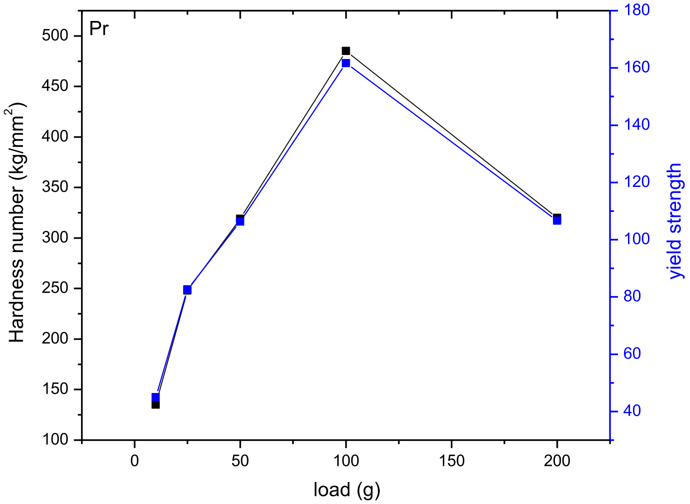

Fig. 20 Load verses hardness number and yield strength of Pr^{3+} doped phosphate glass

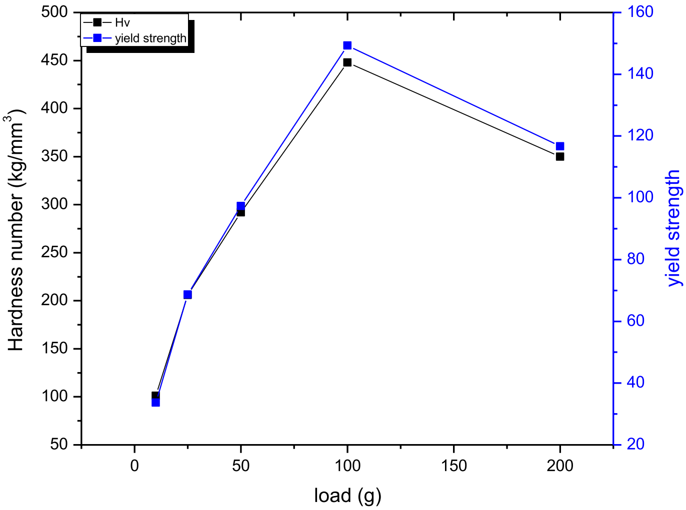

Fig. 21 Load verses hardness number and yield strength of Yb^{3+} doped phosphate glass

$$\sigma_y = \left(H_v/3\right) \text{kg/mm}^2 \tag{20}$$

The work hardening coefficient value (*n*) of the Pr^{3+} and Yb^{3+} doped phosphate glasses were determined from a plot of log P versus log d using Mayer's relation, $P = k_1 d^n$ (Onitsch 1956) and it shows a straight line as shown in Figs. 22 and 23. According to Onitsch, 'n' should lie between 1 and 1.6 for hard materials and above 1.6 for soft materials. The n value of both glasses are above 1.6. Hence Pr^{3+} and Yb^{3+} doped phosphate glasses confirmed that both material belong to soft materials category.

The elastic stiffness constant (C11) for Pr^{3+} and Yb^{3+} doped phosphate glasses were calculated using Wooster's empirical formula $C11 = H^{7/4}$. Figures 24 and 25 show that stiffness constants of $Pr^{3+}$and Yb^{3+}doped phosphate glasses varied with applied load. From the measurement, the stiffness constants of Pr^{3+} and Yb^{3+} doped phosphate glasses are increased upto 100 g. It represent that the binding force between the ions are very strong. The analysis based on the fracture toughness of Pr^{3+} and Yb^{3+} doped phosphate glasses. if $c/a \geq 2.5$ (i.e. the crack system is median or half penny) where a is the length of the half diagonal of the indent. For $c/a < 2.5$ i.e. the crack system is Palmqvist type. The result suggest that nature of crake is median.

The fracture toughness of the material was given by the relation (Anstis et al. 1981),

$$K_c = P/\beta_o C^{3/2}\left(\text{MPa m}^{-1/2}\right) \tag{21}$$

where P is an applied load in kg, c is the crack length measured and β_o is taken as 7 for Vickers's indenter. Figures 26 and 27 show load verses fracture toughness and brittle index of Pr^{3+} and Yb^{3+} doped phosphate glasses. Brittle index of the Pr^{3+} and Yb^{3+} doped phosphate glasses were calculated using the relation (Lawn and Marshall 1979),

$$B_i = H_v/\ K_c\ m^{-1/2} \tag{22}$$

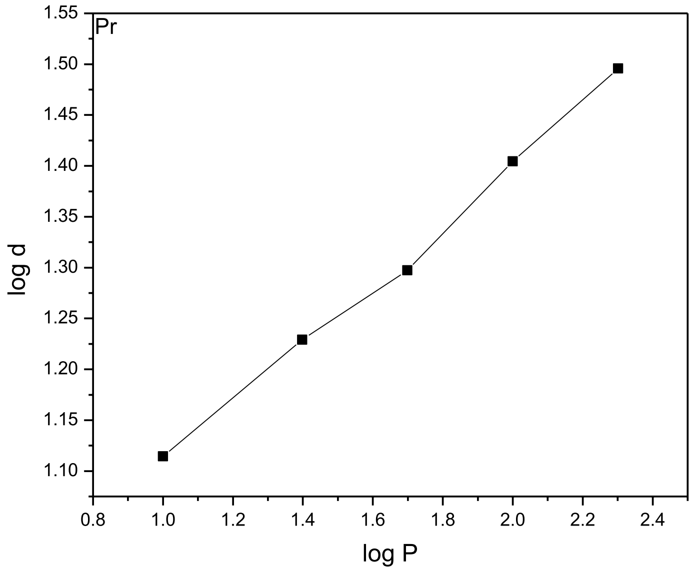

Fig. 22 log P verses log d of Pr^{3+} doped phosphate glass

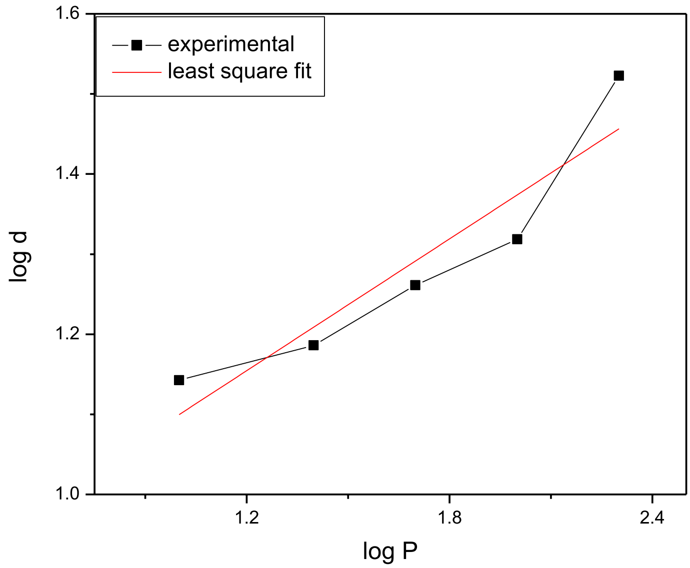

Fig. 23 log P verses log d of Yb^{3+} doped phosphate glass

It is observed that fracture toughness increases with increasing load and brittle index decreased with respect to load. The fracture induced brittleness and affect the mechanical behaviour of the Pr^{3+} and Yb^{3+} doped phosphate glasses. Both glasses have good brittle index.

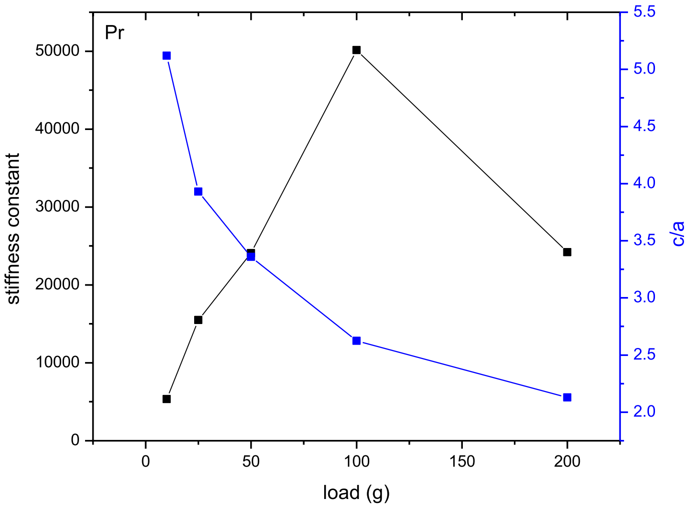

Fig. 24 Load verses stiffness constant and c/a of Pr^{3+} doped phosphate glass

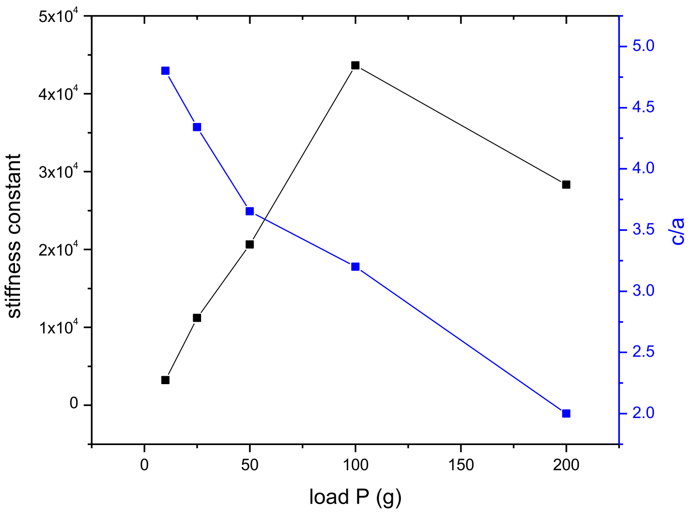

Fig. 25 Load verses stiffness constant and c/a of Yb^{3+} doped phosphate glass

3.5 Vibrating sample magnetometer study

The magnetic property of the Pr^{3+} and Yb^{3+} doped phosphate glasses were studied using VSM analysis at room temperature and hysteresis curves are shown in Fig. 28. From the measurement, the magnetization M linearly depends on applied field.The maximum values of magnetization of occurred at Pr^{3+} and Yb^{3+} doped phosphate glasses were found to be 2.72×10^{-2} emu/g and 2.68×10^{-2} emu/g respectively. While decreasing the field, the M slightly decreases with decreasing H and shows a rentivity 1.134×10^{-3} emu/g and 6.952×10^{-4} emu/g for Pr^{3+} and Yb^{3+} doped phosphate glasses at $H = 0$.

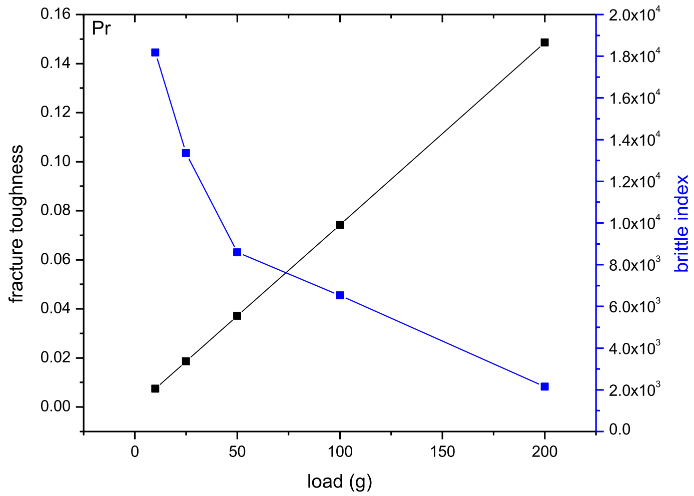

Fig. 26 Load verses fracture toughness and brittle index of Pr^{3+} doped phosphate glass

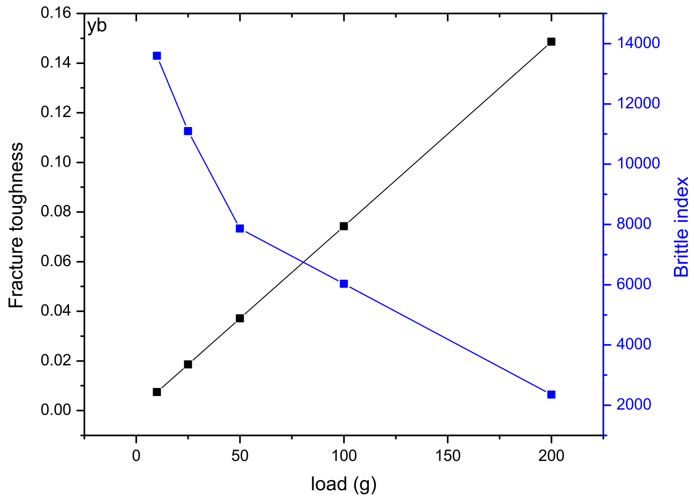

Fig. 27 Load verses fracture toughness and brittle index of Yb^{3+} doped phosphate glass

The magnetization decreases after saturation. This may be due to decrease of spin exchange interaction at higher applied field. For magnetic field of opposite sign, the variation of M shows anomalous property. The M suddenly drops to zero under small magnetic field which denotes a first order metamagnetic transition (Benila et al. 2017; J. Elberin Mary Theras, D. Kalaivani, J. Arul Martin Mani, D. Jayaraman, V. Joseph 2016). The coercivity of the Pr^{3+} and Yb^{3+} doped phosphate glasses are observed to be quite remarkable even though the magnetization is weak and it is found to be 207 G, 205 G respectively. The area of the loop is very steep, so the Pr^{3+} and Yb^{3+} doped phosphate glasses belong to soft magnetic material type.

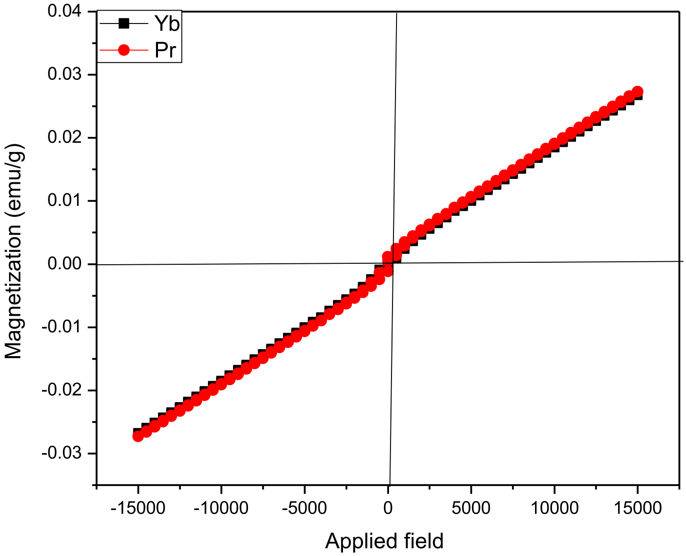

Fig. 28 Hysteresis curves of Yb^{3+} and Pr^{3+}doped phosphate glass

3.6 Electrochemical properties

The Electrochemical properties were carried out for Pr^{3+} and Yb^{3+} doped phosphate glasses with different scan rate in 5 M KOH electrolyte.

The specific capacitances of the cyclic voltammetry measurement (CCV) of the electrodes are calculated by using the relation (Gomez and Kalu 2013; Xiang et al. 2013):

$$C_{CV} = 1/m\upsilon\Delta\upsilon \int IdV \tag{23}$$

where I is the response current (A), υ is the scan rate (mV s-1), m is the mass of the active materials (g), and ΔV is the potential window (V).

The specific capacitance of the galvanostatic charge–discharge measurements (C_{GCD}) of the electrodes was calculated using the equation:

$$C_{GCD} = I\Delta t / m\Delta V \tag{24}$$

where I is the discharge current (A), Δt is the discharge time, m is the mass of the active materials (g), and ΔV is the potential window (V).

The energy density (E) and power density (P) for the electrodes were calculated by the following equations (Khajonrit et al. 2018; Yan et al. 2012):

$$E\,(Wh/\,Kg) = C_{GCD}\Delta V^2/7.2 \tag{25}$$

$$P(W/Kg) = E \times 3600\,/\,t \tag{26}$$

where C_{GCD} is the specific capacitance calculated from charge–discharge measurement (F/g), ΔV is the potential window and t is the discharge time (s). Current density versus specific capacitance of the Pr^{3+} and Yb^{3+} doped phosphate glasses as shown in Fig. 29.

The measurements show that the specific capacitance of the Pr^{3+} and Yb^{3+} doped phosphate glasses decreases with increasing current density. Figure 30 shows the energy density versus power density of the Pr^{3+} and Yb^{3+} doped phosphate glasses.

Yb^{3+} doped phosphate glasses have more specific capacitance and power density than Pr^{3+} doped phosphate glasses. The power density decreases with increase in energy density.

The V-I curves of Pr^{3+} and Yb^{3+} doped phosphate glass was drawn from CV analysis and shown in Fig. 31 and 32 respectively. The oxidatiom peak potential of Yb^{3+} doped phosphate glass is more than Pr^{3+} doped phosphate glass at the scan rate of 80 mV/s.

The nyquist plots drawn between real and imaginary parts of the impedance of Pr^{3+} and Yb^{3+} doped phosphate glasses and shown in Fig. 33. From the measurement, the imaginary impedance increases with respect to real impedance. The end of the curve represent the resistance of the Yb^{3+} and Pr^{3+} doped phosphate glasses at a particular temperature. In general, the glass are ionic or mixed ionic conductor. This resistance may affect the conductivity of the glasses which include network rigidity, network connectivity, the charge, size and mobility of the modifier ions. So the electrochemical performance of the Yb^{3+} doped phosphate is more than Pr^{3+} doped phosphate glass. This result suggest that the Pr^{3+} and Yb^{3+} doped phosphate glass have a potential for development as electrode materials in super capacitor application.

4 Conclusion

The rare earth Pr^{3+} and Yb^{3+} doped phosphate glass were prepared by quenching method using electrical mufulfurnace. The optical parameters such as optical band gap, optical conductivity, refractive index and extinction coefficient of rare earth Pr^{3+} and Yb^{3+} doped phosphate glass were estimated through Uv–Visible spectroscopy analysis. The dielectric permittivity, dielectric loss and electrical conductivity of the prepared

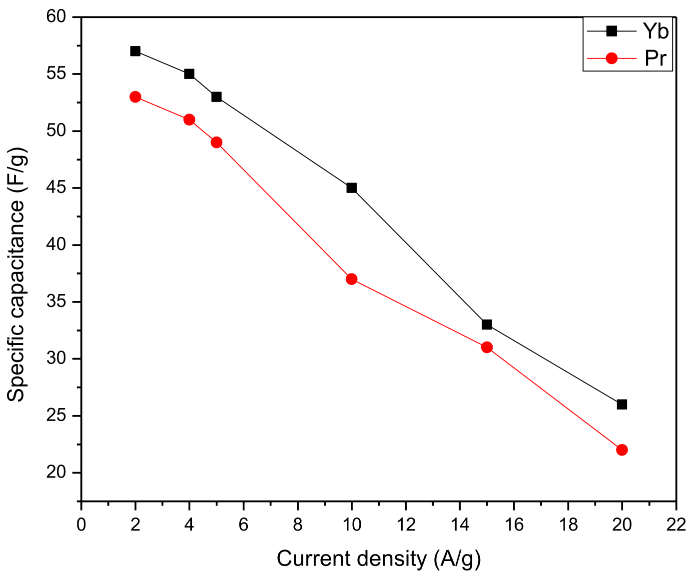

Fig. 29 Current density verses Specific capacitance of the Pr^{3+} and Yb^{3+} doped phosphate glasses

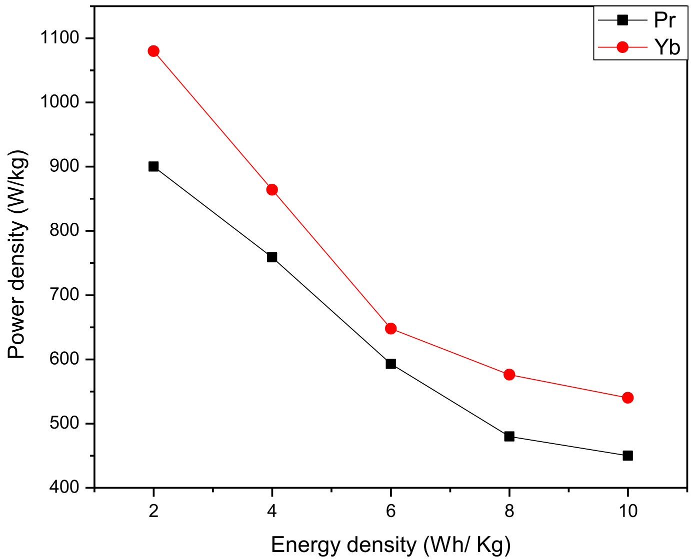

Fig. 30 Energy density verses Power density of the Pr^{3+} and Yb^{3+} doped phosphate glasses

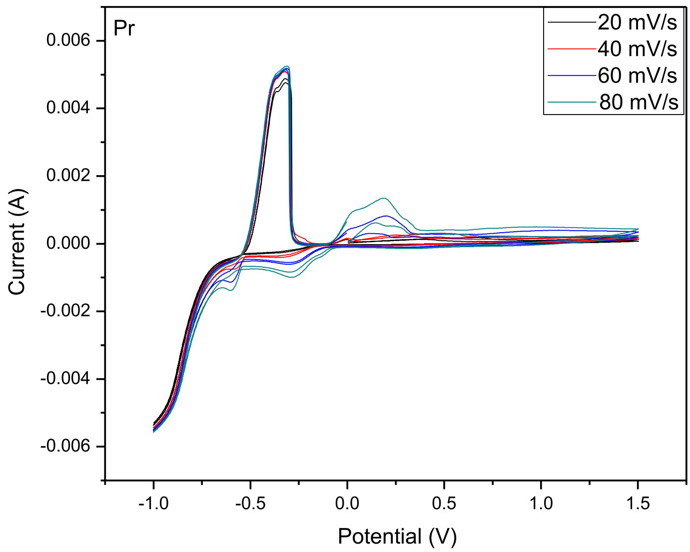

Fig. 31 Potential applied verses Current for Pr^{3+} doped phosphate glass

samples have been studied using LCR meter with different frequencies. The results suggest that the dipoles formed in the glass containing high frequency value are polarized more easily.

The Vickers hardness number, brittle index, yield strength, fracture toughness of the prepared glasses were calculated. The nonlinear optical properties such as third order nonlinear coefficient, nonlinear refractive index were estimated for Pr^{3+} and Yb^{3+} doped

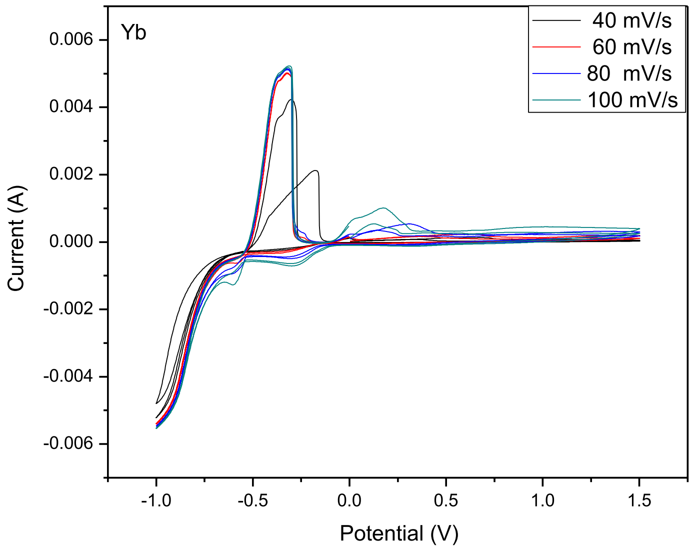

Fig. 32 Potential applied verses Current for Yb^{3+} doped phosphate glass

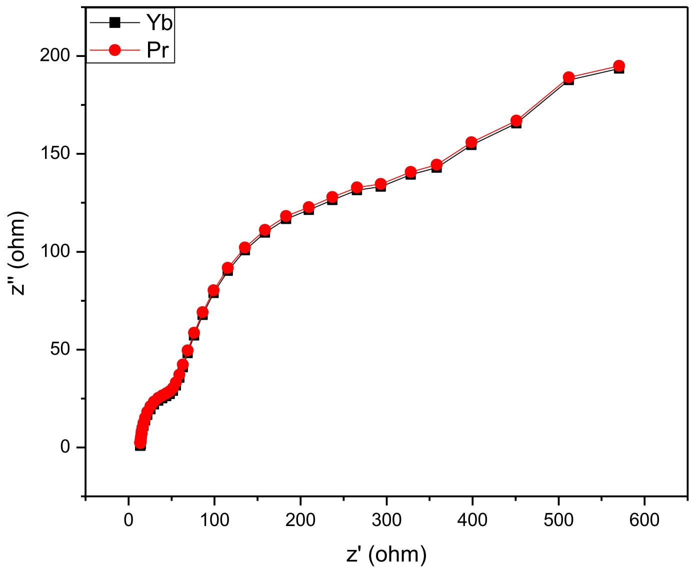

Fig. 33 The Nyquist plot of Pr^{3+} and Yb^{3+} doped phosphate glasses

phosphate glass using Z-scan technique. These studies prove that these type of glasses can be used in nonlinear optical applications.

The coercivity and retentivity of the Pr^{3+} and Yb^{3+} doped phosphate glasses were calculated. The hysteresis loop suggest that the material belong to soft magnetic material category. The energy density (E) and power density (P) of the Pr^{3+} and Yb^{3+} doped phosphate glass were calculated.

Compliance with ethical standards

Conflict of interest The authors declare that they have no conflict of interest.

References

Anstis, G.R., Chantikul, P., Lawn, B.R., Marshall, D.B.: A critical evaluation of indentation techniques for measuring fracture toughness: I. Direct crack measurements. J. Am. Ceram. Soc. **64**(9), 533–538 (1981)

Benila, B.S., Bright, K.C., Mary Delphine, S., Shabu, R.: Optical, thermal and magnetic studies of pure and cobalt chloride doped L-alanine cadmiumchloride. J. Magn. Magn. Mater., **426**:390–395 (2017)

Elisa M., Sava B.A. , Vasiliu I.C., Monteiro R.C.C. , Veiga J.P., Ghervase L., Feraru I., Iordanescu R.: Optical and structural characterization of samarium and europium-doped phosphate glassesA. J. Non-Cryst. Sol.,**369**:55–60 (2013)

Elberin Mary Theras, J., Kalaivani, D., Arul Martin Mani, J., Jayaraman, D., Joseph, V.: Synthesis, structural and optical properties, ferromagnetic behaviour, cytotoxicity and NLO activity of lithium sulphate doped l-threonine. Opt. Laser Technol. **83**: 49–54 (2016)

Gomez, J., Kalu, E.E.: High-performance binder-free Co-Mn composite oxide supercapacitor electrode. J. Power Sources. **230**, 218–224 (2013)

Khajonrit, J., Wongpratat, U., Kidkhunthod, P., Pinitsoontorn, S., Maensiri, S.: Effects of Co doping on magnetic and electrochemical properties of $BiFeO_3$ nanoparticles. J. Magn. Magn. Mater. **449**, 423–434 (2018)

Krishnakumar, V., Nagalakshmi, R.: Crystal growth and vibrational spectroscopic studies of the semiorganic non-linear optical crystal—bisthiourea zinc chloride. Spectrochim. Acta. Part A **61**, 499–507 (2005)

Lawn, B.R., Marshall, D.B.: Hardness, toughness, and brittleness: an indentation analysis. J. Am. Ceram. Soc. **62**(7–8), 347–350 (1979)

Lucarelli, A., Lupi, S., Calvani, P., Maselli, P.: Optical conductivity of the nonsuperconducting cuprate La8−xSrxCu8O20. Phys. Rev. B **65**(054511), 1–7 (2002)

Mojdehi M.S., Yunus W.M.M., Fhan K.S., Talib Z.A., Tamchek N.: Nonlinear optical characterization of phosphate glasses based on ZnO using the Z-scan technique, Chin. Phys. B, 22(**11**):117802–117806 (2013)

Onitsch, E.M.: The present status of testing the hardness of materials. Mikroskopie **95**, 12–14 (1956)

Raja, V., Sharma, A.K., Narasimha, V.V.R.: Impedance spectroscopic and dielectric analysis of PMMA-COP4VPNO polymer films. Mater. Lett. **58**, 3242–3247 (2004)

Rupa, B., Rao, V., Srinivas Prasad, M.V.V.K., Tanuj, K.L., Venkateswarlu, M.: "Spectroscopic Investigations on Pr^{3+} Doped Alkali Fluoroborophosphate Glasses. J. Nanosci. Nanotechnol. **4**(2), 360–363 (2018)

Sadhukhan, M., Modak, D.K., Chaudhuri, B.K.: Study of microstructural behavior and nonadiabatic small polaron hopping conduction in BaTiO3 doped lead-vanadate glass and glass-ceramics dispersed with ferroelectric nanocrystals. J. Appl. Phys. **85**, 3477 (1999)

Sangwal, K.: Review: Indentation size effect, indentation cracks and microhardness measurement of brittle crystalline solids – some basic concepts and trends. Cryst. Res. Tech. **44**, 1019–1037 (2009)

Shanmugavelu, V., Venkatramu, V.V.R.: Kanth, Optical properties of Nd^{3+} doped bismuth zinc borate glasses. Spectrochim. Acta Mol. Biomol. Spectrosc. **122**, 422–427 (2014)

Sharaf L.M., El-Deen, M.S. Al Salhi , Meawad M. Elkholy.: IR and UV spectral studies for rare earths-doped tellurite glasses, J. Alloys Compd., **465**, 333–339 (2008)

Sharma, Y.K., Tandon, S.P., Surana, S.S.L.: Laser action in praseodymium doped zinc chloride borophosphate glasses. Mat. Sci. Eng. **B77**, 167–171 (2000)

Sheik-Bahae, M., Said, A.A., Stryland, E.W.V.: High-sensitivity, single-beam n_2 measurements. Opt. Lett. **14**, 955–957 (1989)

Shelby J. E.: "Introduction to Glass Science and Technology", 2nd Edition (2020)

Ugwu, E.I., Olayinka, A.S., Olabode, F.I.: Analysis of wave propagation in a homogeneous dielectric crystal. J. Eng. Appl. Sci. **4**, 126–131 (2009)

Valente, M.A., Bih, L., Graça, M.P.F.: Dielectric analysis of tungsten–phosphoniobate 20A2O–30WO_3 –10Nb_2O_5 –40P_2O_5 (A = Li, Na) glass ceramics. J. Non-Cryst. Solids **357**, 55–61 (2011)
Xiang, C., Li, M., Zhi, M., Manivannan, A., Wu, N.: A reduced graphene oxide/Co3O4 composite for supercapacitor electrode. J. Power Sour. **226**, 65–70 (2013)
Yakuphanoglu, F., Erten, H.: Refractive index dispersion and analysis of the optical constants of an ionomer thin film. Opt. Appl. **35**, 969–976 (2005)
Yan, J., Liu, J., Fan, Z., Wei, T., Zhang, L.: High-performance supercapacitor electrodes based on highly corrugated graphene sheets. Carbon **50**, 2179–2218 (2012)
Zhang, H., Fu, L., Wang, S., Meng, Q., Yang, K., and Ni, J.: Luminescence characteristics of europium and terbium complexes with 1, 10-phenanthroline in-situ synthesized in a silica matrix by a two-step sol–gel process, Mater. Lett., **38**:260–264 (1999)